How to cite: *Angew. Chem. Int. Ed.* **2023,** *62,* e202214510
International Edition: doi.org/10.1002/anie.202214510
German Edition: doi.org/10.1002/ange.202214510

Homogeneous Catalysis

Iridium-Catalyzed *ortho*-Selective Borylation of Aromatic Amides Enabled by 5-Trifluoromethylated Bipyridine Ligands

Daniel Marcos-Atanes, Cristian Vidal, Claudio D. Navo, Francesca Peccati, Gonzalo Jiménez-Osés, and José L. Mascareñas**

Abstract: Iridium-catalyzed borylations of aromatic C–H bonds are highly attractive transformations because of the diversification possibilities offered by the resulting boronates. These transformations are best carried out using bidentate bipyridine or phenanthroline ligands, and tend to be governed by steric factors, therefore resulting in the competitive functionalization of *meta* and/or *para* positions. We have now discovered that a subtle change in the bipyridine ligand, namely, the introduction of a CF_3 substituent at position 5, enables a complete change of regioselectivity in the borylation of aromatic amides, allowing the synthesis of a wide variety of *ortho*-borylated derivatives. Importantly, thorough computational studies suggest that the exquisite regio- and chemoselectivity stems from unusual outer-sphere interactions between the amide group of the substrate and the CF_3-substituted aryl ring of the bipyridine ligand.

Introduction

The catalytic functionalization of selected C–H bonds in complex organic molecules is a formidable challenge.[1] Despite the impressive progress, the field is yet in its infancy.[2] Many of the efforts in this area have been focused on the functionalization of aromatic C–H bonds owing to the synthetic relevance of the products, and the challenge of distinguishing very similar C(sp^2)–H bonds.[3]

Among the different type of aromatic C–H functionalization reactions, borylations are particularly attractive because of the versatility of the products.[4] A number of rhodium and, particularly, iridium-catalyzed borylation reactions have been studied.[5] These reactions are usually carried out using bidentate 2,2′-bipyridine (bipy) or 1,10-phenanthroline ligands, Ir^I pre-catalysts, and bis(pinacolato)diboron (B_2pin_2) or pinacolborane (HBpin) as reactants. The accepted mechanism of the process involves a catalytic cycle with Ir^{III} and Ir^V intermediates like those showed in Figure 1a, and a rate determining oxidative addition of the C–H bond to the metal.[6] The regioselectivity is usually controlled by steric effects, which tend to favour the functionalization of *meta* and/or *para* positions in benzene derivatives.[7]

Ortho-selective borylation of arenes are more challenging, even in precursors featuring a directing group (DG), because coordination of this substituent to complex **A** leads to a fully saturated iridium complex (18 electrons) unable to participate in the oxidative addition step. Some groups have overcome this limitation by using monodentate phosphines,[8] or hemilabile bidentate ligands.[9] However, these ligands are usually less efficient than bipyridines and phenanthrolines in promoting the C–H activation, and tend to favor the formation of off-cycle species.[10] Alternatively, the reactions can be performed using specifically engineered monoanionic bidentate L,X -type ligands, in which the anionic part (X) replaces one of the boron groups in intermediate **A**, and therefore coordination of the DG to the iridium atom is now possible.[11]

Recently, some elegant strategies for the *ortho* borylation of electron rich aromatics based on non-covalent interactions between the Ir reagent and the substituent of the arene have been developed (Figure 1b).[12] These include hydrogen bond contacts (Figure 1b, **B**),[13] or electrostatic interactions between the oxygen of an OBpin group and the bipyridine ligand (**C**).[14] With some exceptions,[12b] substrates lacking substituents at the *para* position tend to give mixtures of products, presumably because the weak outer-sphere interactions do not fully override the intrinsic sterically-driven regiocontrol.

Kuninobu and Kanai described the *ortho* borylation of phenyl thioethers, proposing a Lewis acid-base interaction between the S atom and either a boronate pendant, or the B atom of one of the Bpin groups attached to the iridium (Figure 1b, **D**, **E**).[15]

[*] D. Marcos-Atanes, Dr. C. Vidal, Prof. Dr. J. L. Mascareñas
Centro Singular de Investigación en Química Biolóxica e Materiais Moleculares (CIQUS), and Departamento de Química Orgánica, Universidade de Santiago de Compostela
15782 Santiago de Compostela, A Coruña (Spain)
E-mail: joseluis.mascarenas@usc.es

Dr. C. D. Navo, Dr. F. Peccati, Dr. G. Jiménez-Osés
CIC bioGUNE, Basque Research and Technology Alliance, BRTA
Bizkaia Technology Park, 48162 Derio (Spain)
E-mail: gjoses@cicbiogune.es

Dr. G. Jiménez-Osés
Ikerbasque, Basque Foundation for Science, 48013 Bilbao (Spain)

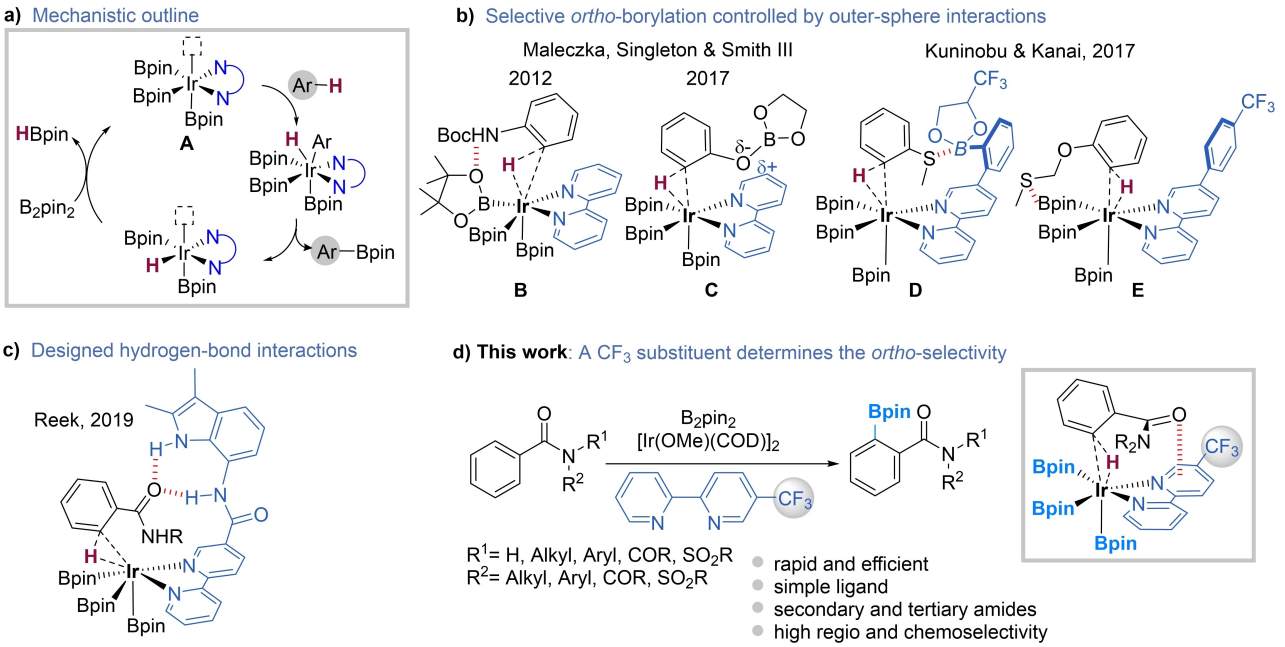

Figure 1. a) Accepted mechanistic profile for the iridium-catalyzed borylation reactions; b) Previous works on directed *ortho*-borylations controlled by outer-sphere non-covalent interactions; c) H–bond directed, *ortho*-borylation of secondary benzamides; d) Strategy presented in this manuscript.

A very attractive type of substrates for C–H bond borylation are benzamides, as they form the core of many compounds with valuable properties.[16] However, robust and versatile methods for the direct *ortho* borylation of different types of benzamides are scarce. Reek and co-workers described a tailored bipyridine derivative that is capable of inducing the *ortho* borylation of *N*-methyl and *N*-benzyl benzamides (Figure 1c).[17] The strategy relies on an engineered bipyridine–indole ligand, and the scope is restricted to secondary amides.

Very recently, Chattopadhyay and co-workers reported the use of monoanionic bidentate L,X-type ligands to promote *ortho*-selective C–H bond borylation of a variety of benzamides.[11c] This approach is also compatible with substrates containing other directing groups. However, this poses a limitation to performing chemoselective transformations in complex settings where numerous functional groups are present. Indeed, in heteroaromatic substrates the directing effect of the carboxamide is overridden by the intrinsic electronics of the heterocycles.

As part of our research in C–H activation chemistry,[18] we have now discovered that introducing a CF_3 substituent in position 5 of a 2,2′-bipyridine ligand induces a complete change in regioselectivity in the borylation of aromatic amides from *meta/para*- to *ortho*-selective. The change in selectivity by such a subtle change in a L,L-type of ligand is intriguing, and therefore we conducted a detailed experimental and computational study to uncover the underlying basis for the directing effect. Our results suggest that the selectivity originates from unusual non-covalent attractions between the benzamide group of the substrate and the bipy-CF_3 ligand (Figure 1d).

Results and Discussion

Influence of the Bipyridine Substituents in the Borylation

Our interest in this reaction was prompted by the observation that the borylation of *N,N*-dimethylbenzamide (**1a**) under iridium catalysis led to a different result when moving from the standard bipyridine ligand to one that contains a phenyl substituent at the 5 position of one of the pyridines. The reaction with the common ligands 4,4′-di-*tert*-butyl-2,2′-bipyridine (dtbpy, **L1**) and 2,2′-bipyridine (bipy, **L2**) produced a mixture of *meta* and *para* mono- and diborylated products (Table 1, entry 1, 2).[19] However, using the phenyl containing ligand **L3**, we observed a small amount of the *ortho*-substituted product (entry 3), which further increased when using **L5** (entry 5).

Replacing the aryl by a methyl substituent in the bipyridine (**L6**, entry 6) led to a similar result than with 2,2′-bipyridine, whereas with halogen substituted bipyridines (**L7** and **L8**) we observed a slightly higher *ortho*-borylation (entries 7, 8). Surprisingly, when a CF_3 substituent was introduced (ligand **L9**), we observed the exclusive formation of *ortho* mono- and diborylated products (entry 9). Ligands with other electron-withdrawing substituents at position 5, such as **L10** (C_6F_5) and **L11** (CN), also afforded the *ortho*-borylated compounds as the major products, but were less selective than **L9**, and the detected diborylated products consisted of mixtures of regioisomers (entries 10 and 11).

With **L12** (entry 12), featuring a CHF_2 substituent, we also observed mixtures, with partial *ortho* borylation. The perfluorinated derivative (**L13**, entry 13) and the symmetric ligand **L14**, with CF_3 substituents at the 5 positions of each

Table 1: Ligand effects on regioselectivity.[a,b]

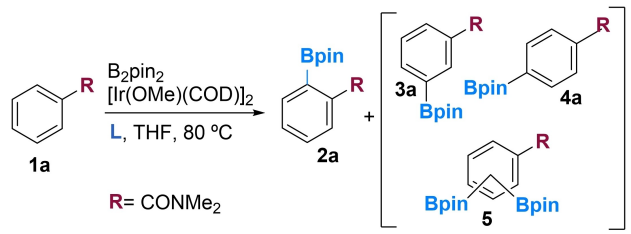

Entry	L	Conv [%]	2a [%]	3a [%]	4a [%]	5 [%]
1	**L1**	100	0	18	30	52
2	**L2**	99	0	28	37	34
3	**L3**	99	14	28	11	53
4	**L4**	99	11	25	10	53
5	**L5**	98	42	11	3	42
6	**L6**	99	4	35	23	37
7	**L7**	99	4	31	19	45
8	**L8**	87	12	40	23	12
9	**L9**	100	20	0	0	80[c]
10	**L10**	100	49	3	1	47
11	**L11**	99	46	4	2	47
12	**L12**	98	28	27	13	29
13	**L13**	100	62	0	0	38[c]
14	**L14**	100	19	0	0	81[c]
15	–	8	8	0	0	0
16[d]	**L9**	97	90 (83)	0	0	7
17[d]	**L15**	58	58	0	0	0

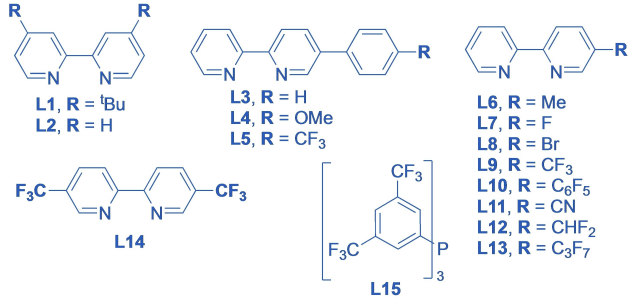

Reaction conditions: [a] **1a** (0.25 mmol), B_2pin_2 (0.375 mmol, 1.5 equiv), $[Ir(OMe)(COD)]_2$ (3 mol%), L (6 mol%), THF (0.2 M), 80 °C, 3 h. [b] Diborylated product 5 consists of a mixture of isomers, unless otherwise stated. [c] Exclusively the di-ortho-borylated regioisomer. [d] 65 °C for 1.5 h, isolated yield of **2a** in parenthesis. Note: Conversion and % of products were determined by GC/MS analysis. For more details about 5 isomers see the Supporting Information (Table S1).

ring also led to *ortho* products (entry 14). These results suggest that the stereoelectronic characteristics of the CF_3 group are especially effective in imparting the desired regiocontrol. *Ortho*-borylation was also detected even when no ligand was used (entry 15), but conversion was much lower.[11d]

The optimized conditions for the *ortho* borylation using **L9** as ligand consists of: 1 equiv benzamide, 1.5 equiv B_2pin_2, 3 mol% $[Ir(OMe)(COD)]_2$ and 6 mol% **L9** in THF (0.2 M) at 65 °C, and gave product **2a** after 1.5 hours in 83% yield, with only 7% yield of the diborylated byproduct (entry 16).

With the electron-deficient phosphine ligand **L15**, which is known to favor *ortho* borylations by allowing a direct coordination of the carbonyl group to the metal,[8] product **2a** was also formed; however, the reaction was slower and less efficient than with **L9** (58% yield after 1.5 h, entry 17).

As an initial hypothesis to explain the striking effect of the CF_3 substituents at C-5, we considered that electron deficient bipyridine ligands might favor the formation of Ir^I complexes, and therefore change the catalytic process from the standard Ir^{III}/Ir^V cycle to one involving Ir^I/Ir^{III} intermediates, which might allow chelation of the amide. However, when running the reaction with positional isomers **L16** and **L17**, we observed lower conversions and the formation of *meta* and *para*-substituted products (Figure 2). This drastic change in reactivity and regioselectivity by just moving the CF_3 groups from the *meta* to the *ortho* or *para* positions in the bipyridine is astonishing, and raised intriguing mechanistic questions.

Kinetic Studies

To gain mechanistic insights, we performed comparative kinetic studies using the standard bipyridine **L2**, and the CF_3-substituted derivatives **L9** and **L17**. Ligand **L9** leads to almost full conversion after 1.5 h at 65 °C, generating the *ortho* borylated product exclusively, while the borylations with **L2** and **L17**, which yielded a mixture of *meta* and *para* borylated products, are faster and slower respectively (Figure 3a).

Monitoring the reactions kinetics at different temperatures revealed substantially different apparent activation enthalpies ($\Delta H^{\ddagger}_{obs}$) and entropies ($\Delta S^{\ddagger}_{obs}$) for the reactions carried out with **L9**, than for those involving **L2** or **L17** (Figures S1–S5). These dissimilar numbers in the activation parameters depending on the ligand, are likely associated to

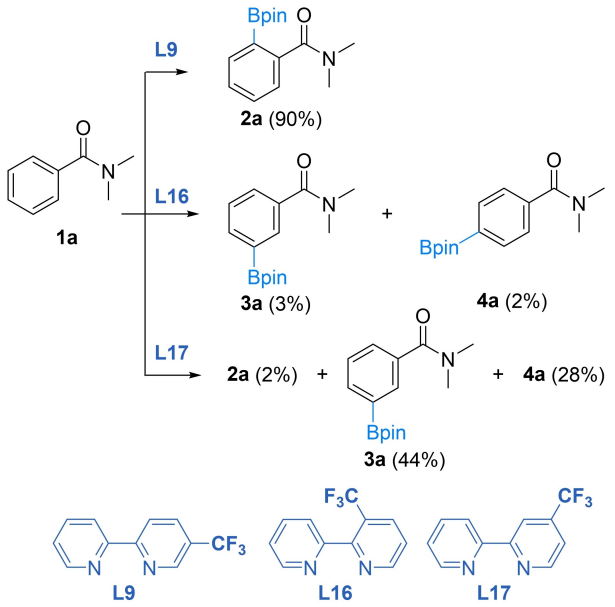

Figure 2. Regioselectivity changes depending on the position of the CF_3 substituents in the bipy ligand. Reaction conditions: **1a** (0.25 mmol), B_2pin_2 (0.375 mmol, 1.5 equiv), $[Ir(OMe)(COD)]_2$ (3 mol%), ligand **L** (6 mol%), THF (0.2 M), 65 °C, 1.5 h.

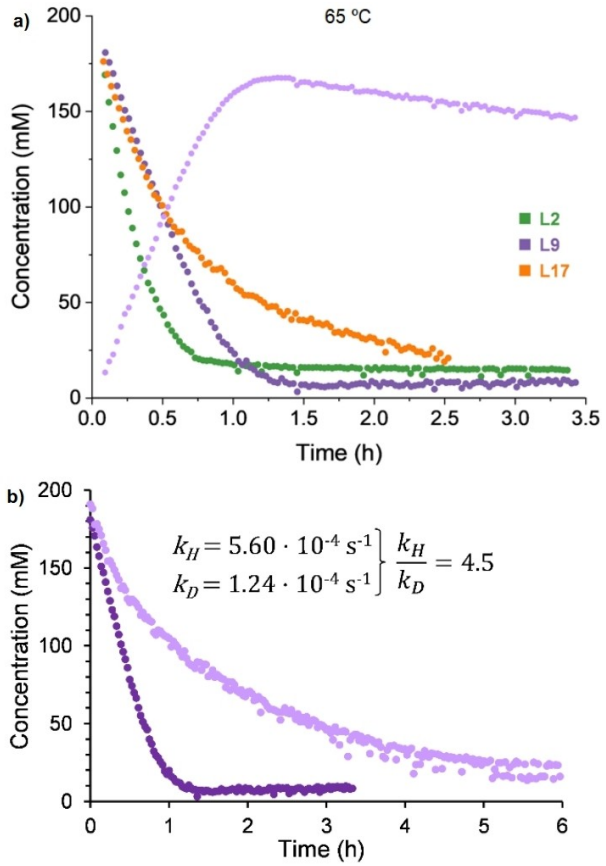

Figure 3. a) Reaction monitoring using different ligands. Conversion of substrate **1a** with ligands **L2** (green), **L9** (dark purple) and **L17** (orange), and formation of *ortho*-monoborylated product **2a** with ligand **L9** (light purple) are shown. b) Kinetic isotope effect (KIE) determined from parallel reactions of substrates **1a** (dark purple) and **1a**-d_5 (light purple).

different stabilities of precatalytic iridium species formed in the initial reaction mixture,[6] but they are not necessarily informative on the origin of the regioselectivity.

Importantly, parallel kinetic experiments using **1a** and its d_5-deuterated analogue as substrates, and **L9** as a ligand, revealed a KIE of 4.5, similar to that obtained with bipy (**L2**),[6a] and consistent with a canonical mechanism involving a turnover-determining C–H activation (Figure 3b).

Solvent Effects

We also evaluated the effect of different solvents on the reaction outcome (Table S2). Non-polar hydrocarbon solvents like hexane or cyclohexane decreased reactivity, and, remarkably, led to regioisomeric mixtures. Weakly polar ethereal solvents such as dibutyl ether led to a different result than the more polar THF, with formation of *meta* and *para* borylated products as major products. Therefore, there is an important influence of the solvent in the regioselectivity, which started to suggest the existence of non-covalent interactions in the regio-determining step.

Reaction Scope

Before going into further mechanistic details, it was essential to find out whether the *ortho*-borylation reaction can be generalized. Gratifyingly, many other tertiary amides participated in the process (Scheme 1). *Ortho*-monoborylated products **2a**–**2g** were obtained in high yields and excellent regioselectivities, as no other mono-borylated side products were detected when using **L9** as a ligand. As expected, using **L2** instead of **L9**, we did not detect *ortho*-borylated products, but only mixtures of other regioisomers (See Supporting Information for more details, Figure S9).

The results obtained with amides featuring phenyl substituent at the nitrogen atom (**1c**, **1i**), which pose a chemoselectivity challenge (i.e. two aryl rings can be functionalized), are remarkable. Using **L2** we observed mixtures of *meta* and *para* substituted products in the

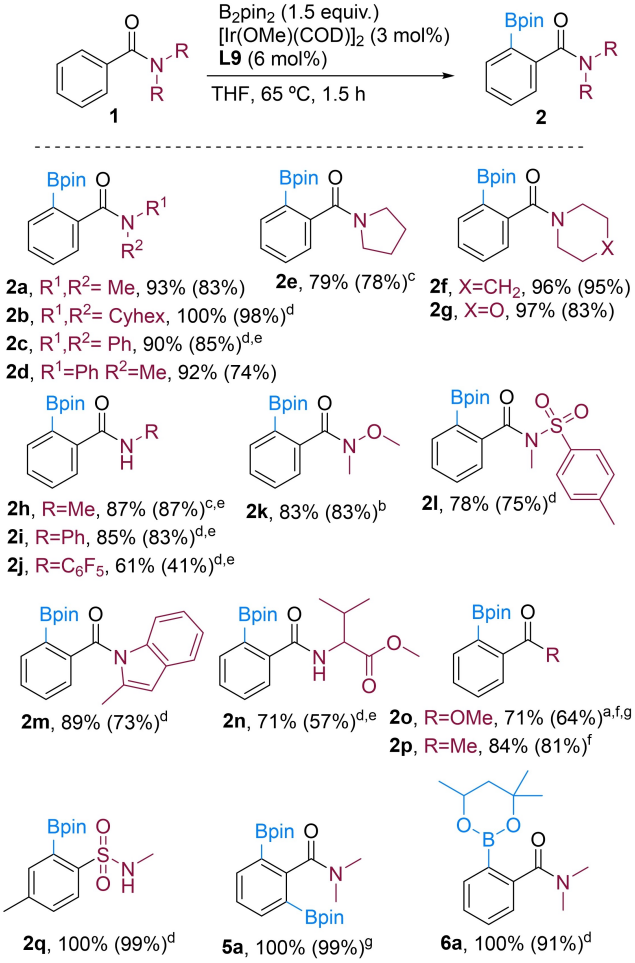

Scheme 1. Borylation of benzamides and related precursors. Reaction conditions: substrate (0.25 mmol), B_2pin_2 (0.375 mmol, 1.5 equiv), $[Ir(OMe)(COD)]_2$ (3 mol%), **L9** (6 mol%), THF (0.2 M), 65 °C, 1.5 h. ^1H NMR yield using CH_2Br_2 as IS (mean value of 3 parallel reactions), isolated yield described between parenthesis [a] Reaction time 1 h. [b] Reaction time 2 h. [c] Reaction time 4 h. [d] Reaction time 24 h. [e] Reaction temperature 80 °C. [f] Reaction temperature 100 °C. [g] Ligand **L14** was used. Note: only traces of diborylated products were detected.

benzamide ring, and partial borylation of the phenyl substituent attached to the N atom. However, with **L9**, the reaction was completely chemoselective towards the benzamide phenyl ring (products **2c** or **2d** were obtained in excellent yields).

We were pleased to find that the reaction also works with secondary amides, affording *ortho* borylated products **2h**–**2j** in good yields. As with tertiary benzamides, the presence of additional phenyl rings in the substrates was tolerated, if ligand **L9** is used. Interestingly, a C_6F_5 substituent at the nitrogen slowed down the reaction, suggesting an important effect of the stereoelectronic properties of the amide on the reaction rate. Other heteroatom substituents at the nitrogen such as –OMe (Weinreb amide) or –SO_2–R, are also compatible, and products **2k** and **2l** could be formed in good yields with no other borylation products detected. The same chemoselectivity was observed with a substrate featuring an indole moiety (**2m**). The amino acid containing product **2n** was also produced with high selectivity, which suggests that the method might be used for late-stage functionalization of short peptides with benzamide substituents.

Overall, our results confirm that the *ortho*-borylation is widely applicable. Control reactions with some of these substrates using **L2** instead of **L9** as a ligand, failed to give the *ortho*-borylated products (Figure S9). When B_2pin_2 was replaced with bis(hexyleneglycolato)diboron we obtained the expected product **6a**. As discussed before, the *ortho*-diborylated product **5a** can be obtained using **L14** and an excess of B_2pin_2.

The observed reactivity is not limited to benzamides; methylbenzoate reacted to give the *ortho* borylation product **2o**, although the reaction required heating up to 100 °C and the use of ligand **L14**. Acetophenone also reacted to give the expected product, with only traces of a secondary hydroborylation. In addition, *N*-Me-tosylsulfonamide was an effective substrate for the reaction, obtaining the expected product **2q** in excellent yield. When bipyridine (**L2**) was used as a ligand no *ortho* borylation was observed.

Ortho-borylation is effective on benzamides exhibiting different types of substituents at the aryl ring. The reaction is successful with substrates featuring both EDG (–Me or –OMe) or EWG (–CF_3) *para* to the amide, giving the expected products (**2aa**–**2ac**) in good yields (Scheme 2). Halogen groups such as –Cl and –Br, which might be sensitive to the metal reagent, were also tolerated. Importantly, the reaction can also be performed in the presence of unprotected alcohols or amines (products **2af** and **2ag**). *Meta*-substituted precursors also react, to give products borylated at the less hindered *ortho* position relative to the amide group, as in **2ai** and **2aj**. Substrates bearing *ortho* substituents, which have proven difficult to functionalize in the past,[11c] reacted very efficiently to give the expected products (**2ak**–**2an**) in excellent yields.

Disubstituted benzamides also gave the expected *ortho* borylated products (**2ao**–**2aq**). It is important to note that when using **L2** as a ligand many of these functionalized precursors underwent poor conversions (likely because of steric hinderance) and gave mixtures of products (*meta*-substituted, see Figure S9). Therefore, 3,5-dimethoxy-*N*,*N*-dimethylbenzamide failed to react using **L2** as a ligand; however, **L9** led to good yields of the expected products (**2ao**).

Interestingly, 2,6-dimethyl-*N*,*N*-dimethylbenzamide (*ortho*-disubstituted amide) led to no conversion (**2as**) under standard conditions with **L9**; however, with **L2** we observed the *para*-borylated product with excellent conversions (See Figure S9). Along the same lines, it is important to highlight that substrates like anisole or toluene remained essentially unchanged under standard conditions in the presence of **L9**. However, they react in the presence of **L2** (65 °C, 1.5 h),[19] to give *meta*/*para* borylation products (See Table S4). When

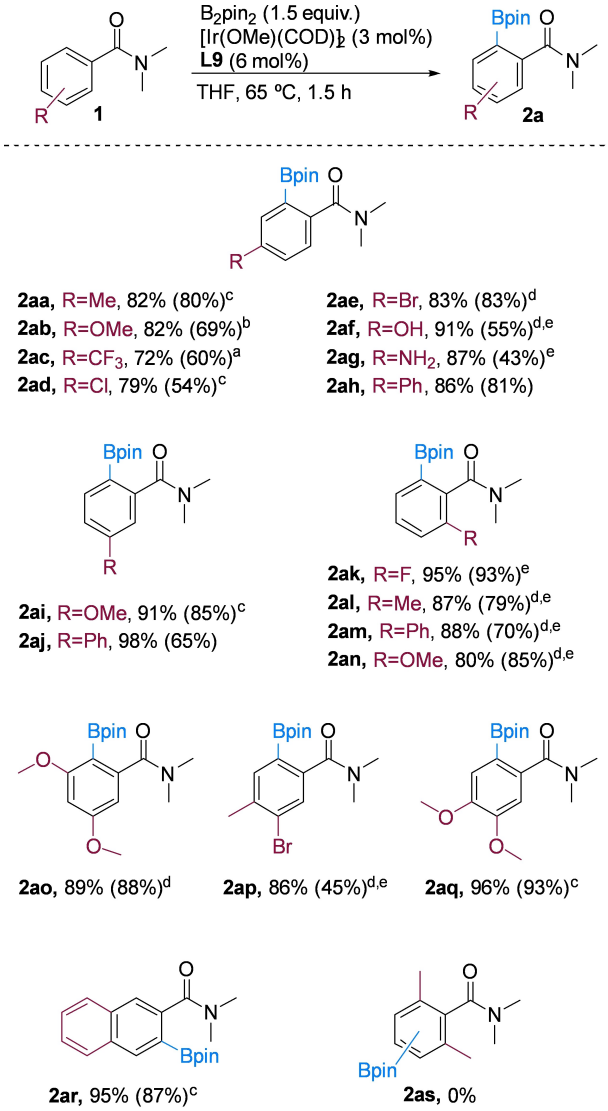

Scheme 2. Borylation of substituted benzamides. Reaction conditions: substrate (0.25 mmol), B_2pin_2 (0.375 mmol, 1.5 equiv), $[Ir(OMe)(COD)]_2$ (3 mol%), **L9** (6 mol%), THF (0.2 M), 65 °C, 1.5 h. ^{1}H NMR yield using CH_2Br_2 as IS (mean value of 3 parallel reactions), isolated yield described between parenthesis. [a] Reaction time 1 h. [b] Reaction time 1.25 h. [c] Reaction time 2 h. [d] Reaction time 24 h. [e] Reaction temperature 80 °C. Note: only traces of diborylated products were detected.

the reaction with **L9** is carried out at higher temperatures (100 °C) we start to see reactivity, to give the same regioisomers than with **L2**.

All these results confirm that with **L9** the reaction is both chemo- (only substrates bearing a substituted carbonyl/sulfonyl directing group work), and regioselective (*ortho* orientation). Other substrates lacking a proper carbonyl-like directing group failed to undergo the *ortho*-borylation (see Supporting Information).

Interestingly, phthalimide and naphthalimide reacted in presence of **L9**, but to give the *meta* and the *para* borylated products, respectively, with no *ortho*-borylation. These results may be explained by the rigid planar conformation of the carbonyl group (see Supporting Information).

Precursors with extended aromatic systems were also borylated only at the *ortho* position of the amide group. Therefore, the *ortho*-borylated biphenyl amides **2ah**, **2aj** and **2am** were obtained in excellent yields when using **L9**, whereas with **L2** we observed mixture of products. Likewise, a naphthalene amide substrate was borylated at the *ortho* position of the amide (**2ar**).

Next, we assessed whether the *ortho* borylations could be extended to challenging heterocyclic systems containing amide functionalities. As shown in Scheme 3a, the reaction proceeds with excellent yields on different heterocycles such as indoles (**2r**), pyrroles (**2s** and **2t**), furans (**2u**), and even thiophenes (**2v**). Importantly, in all the cases, the regioselectivity of the reaction is governed by the amide directing group, which contrasts with related borylations using other ligands.[11c]

The data presented above supports a highly regio- and chemoselective transformation, with the substituted amide playing a key role as reaction-promoting and *ortho*-directing group, when combined with ligand **L9**. In agreement with the prevalent directing effect of the amide, we observed that disubstituted precursors containing other potential directing groups, gave exclusively mono-borylated products *ortho* to the amide (**2at**–**2aw**). A substrate exhibiting competing dimethyl and diphenyl amides gave the product borylated *ortho* to the dimethyl amide (**2ax**).

More complex substrates like indomethacine (**7**), benzocaine (**9**), or the insect repellent **11**, can also be borylated with excellent selectivity using **L9**, while the reaction with **L2** affords a mixture of products borylated at multiple positions (Scheme 4). Overall, the chemo and regiodirecting effect of CF_3-containing ligand **L9** is very robust and covers a wide variety of substrates.

Synthetic Application

Finally, the synthetic potential of the method is underscored by its application to a straightforward synthesis of fungicide **14** (43 % overall, only two synthetic operations, (Scheme 5)), while the patented process involves 5 different steps, and it is less efficient.[21]

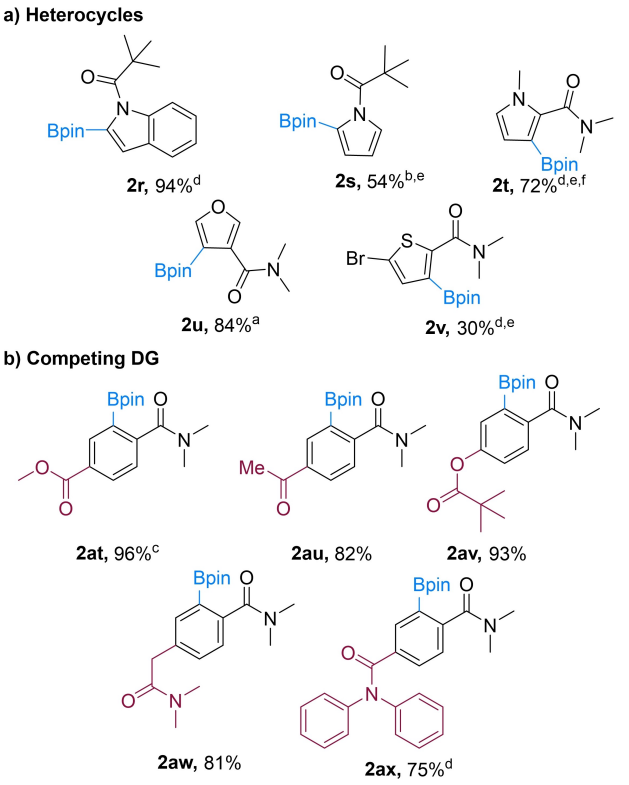

Scheme 3. Borylation of heterocycles, and of substrates with competing DGs (directing group). Reaction conditions: substrate (0.25 mmol), B_2pin_2 (0.375 mmol, 1.5 equiv), [Ir(OMe)(COD)]$_2$ (3 mol %), **L9** (6 mol %), THF (0.2 M), 65 °C, 1.5 h. Isolated yields. [a] Reaction time 15 min. [b] Reaction time 1 h. [c] Reaction time 2 h. [d] Reaction time 24 h. [e] Reaction temperature 80 °C. [f] Ligand **L14** was used a) Borylation of heterocyclic substrates. b) Chemo- and regioselective borylations demonstrate the selectivity of the amide moiety over competing DG.

Computational Assessment of the C–H Activation Step

The clean selectivity outcomes of the above borylations suggest a key role for the amide group in the C–H activation step. However, a direct interaction of this group with the Ir^{III} reagent (complex **A** in scheme 1) saturates the metal center, and would hamper the C–H activation.

To gain further insights into the origins of the observed *ortho* regioselectivity with **L9** we performed a thorough quantum mechanical study on the C–H activation step (see computational details in the Supporting Information).

First, the possibilities that an electron deficient bipy ligand such as **L9** could enable an Ir^{I}/Ir^{III} mechanistic pathway (Figures S11 and S12), or act as an hemilabile ligand allowing direct coordination of the amide to the metal,[9] were discarded due to the very high activation barriers calculated for the C–H activation ($\Delta G^{\ddagger}_{ortho}$ = 43–51 kcal mol^{-1}, Figure S13). Importantly, the barriers when decoordinating the pyridine ring in **L9** are similar to those calculated with **L2**.

We therefore focused our attention on a canonical C–H activation mechanism, with bipyridines acting as bidentate ligands (Figure 1a). Off-cycle Ir^{III} and Ir^{V} complexes with

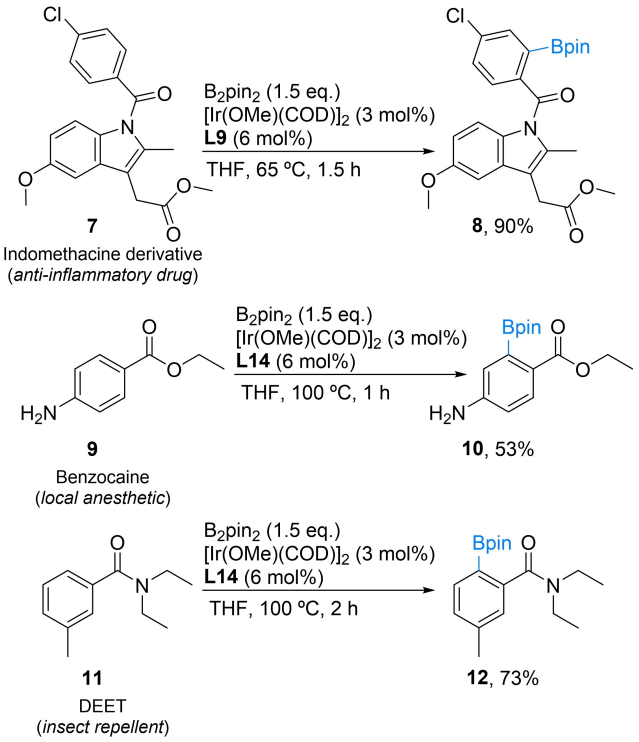

Scheme 4. Borylation of biologically-relevant molecules.

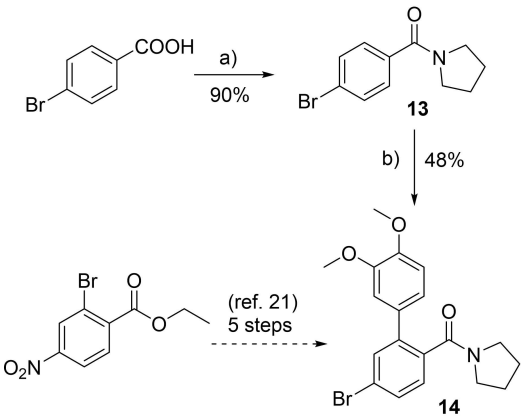

Scheme 5. Three step-synthesis of fungicide **14**. a) $(COCl)_2$ (1.5 equiv), DMF, CH_2Cl_2, 0 °C to r.t., 2 h; then pyrrolidine 0 °C to r.t., 16 h; b) B_2pin_2 (1.5 equiv), $[Ir(OMe)(COD)]_2$ (3 mol%), **L9** (6 mol%), THF, 65 °C, 1.5 h; then H_2O, degassed and $Pd(PPh_3)_4$, K_2CO_3, 3,4(dimethoxy)iodobenzene, 100 °C, 16 h.

either three Bpin and one THF molecule (**L2_THF** and **L9_THF**) or five Bpin units (**L2_IrV** and **L9_IrV**) coordinated to Ir, were calculated to be energetically feasible (Figure S15). These 18 electron species in equilibrium could be considered as catalyst resting state(s) before the TOF-determining C–H activation step, affecting the effective concentration of the reactive catalyst and thus the global reaction rate.[22] The calculations indicate that complexes with ligand **L9** are systematically more stable than those with **L2**. This might be the reason behind the relatively large activation enthalpy and more favorable activation entropy observed for **L9**. More stable saturated species could impose an enthalpic penalty to the C–H activation, while their necessary dissociation of some ligand to form the active catalyst might provide an entropic driving force.

We then analyzed the C–H activation step in detail by considering all possible regioisomers (*ortho*, *meta* and *para*), and conformers of relevant stationary points at each potential energy surface (Figures S13 to S17). Importantly, the $Ir^{III}(bipy)(Bpin)_3$ complexes entering the catalytic cycle are considerably more stable (>4 kcal mol^{-1}) when bound to the substrate via agostic C–H···Ir interactions (**L2_RC** and **L9_RC**), than when coordinated to the amide carbonyl (**L2_RC$_{DG}$** and **L9_RC$_{DG}$**).

Regarding the regioselectivity-determining transition states, the computed activation energies (≤ 30 kcal mol^{-1}) and $^2D/^1H$ KIEs with ligand **L9** (Figure S8), agree with the observed reactivity. Most importantly, only ligand **L9** showed a clear preference for oxidative addition at *ortho* vs. *meta* or *para* positions (calculated *o*:*m*:*p* ratio = 81:15:4, Figure 4). On the contrary, for the isomeric trifluoromethylated ligands **L16** (calculated *o*:*m*:*p* ratio = 31:67:2) and **L17** (calculated *o*:*m*:*p* ratio = 26:73:0), the *meta*-borylation was preferred. This was also the case with unsubstituted bipyridine **L2** (calculated *o*:*m*:*p* ratio = 6:94:0). Overall, these trends are in consonance with the observed selectivities.

The Role of Non-Covalent Interactions on the Regioselectivity of the C–H Activation

A close inspection of the calculated structures reveals that although the geometry of the lowest energy *ortho* and *meta* TS with ligands **L2** and **L9** are almost identical (Figure 4), their relative energies are significantly different, leading to an inversion of regioselectivity. This strongly suggests that outer-sphere substrate-ligand non-covalent interactions in the *ortho* oxidative addition transition states drive the regioselectivity. Exhaustive non-covalent interaction analyses (Figures 5, S24–S28 and Tables S6–S9) unveiled an extended network of attractive interactions between the carbonyl group of the benzamide and the CF_3-pyridine ring of ligand **L9** in the *ortho* TS; these interactions are weaker for the unsubstituted bipyridine ligand **L2** (Figure 5).

NBO[23] analysis suggests that dispersion contacts between the amide carbonyl group and the CF_3-pyridine ring of **L9** (especially the interaction $\pi_{C=O} \rightarrow \pi^*_{C-C}$) are predominant (Figure S25), resulting in a shorter CO···CC distance and a more stable transition structure (**L9_TS_*o***) than with **L2** (**L2_TS_*o***, Figure 5). The polarizing (i.e. electron withdrawing) effect of the CF_3 substituent in **L9** (Figure S29), exacerbates the intensity of outer-sphere substrate-ligand attractions, which seems key for the preferred *ortho* orientation. This was confirmed by an energy decomposition analysis of these interactions (EDA, Figure S26), which suggests that both polar, but especially dispersion contributions increase with ligand **L9**. The calculated non-covalent interactions appear to involve also contacts between the

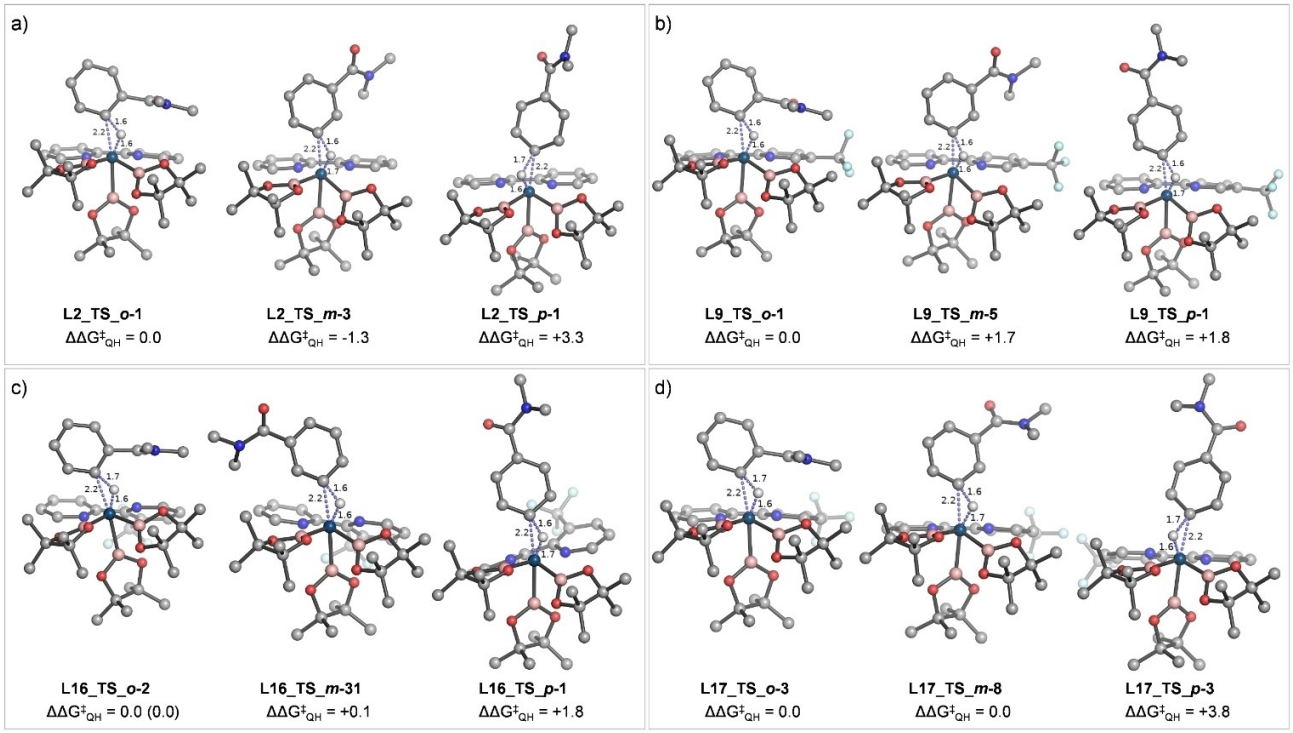

Figure 4. Low energy outer-sphere transition states (TS) calculated for the oxidative addition step between *N*,*N*-dimethylbenzamide (**1a**) and Ir^{III}(ligand)(Bpin)$_3$ (ligand = **L2** (a), **L9** (b), **L6** (c) and **L17** (d); ***o*** = *ortho*, ***m*** = *meta*, ***p*** = *para*). Relative activation free energies ($\Delta\Delta G^{\ddagger}_{QH}$) calculated with SMD_{THF}/M06/6-311G(2d,p) + SDD(Ir)//M06/6-31G(d) + LANL2DZ(Ir) are given in kcal mol^{-1}. Metal-ligand and breaking/forming C–H, Ir–C and Ir–H bonds are represented as blue dashed lines, respectively. Non-reactive hydrogens have been omitted for clarity.

amide substituents and the CF_3 group at position 5 (Figures 5, S24 and S28). On the contrary, in the other CF_3-containing ligands, the more distal location of the CF_3 group in **L17** or the deplanarization of the bipy-Ir chelate in **L16**, reduce the intensity of substrate-ligand interactions in the TS, and thus the *ortho*-selectivity vanishes, as observed experimentally.

Importantly, our model is fully consistent with the absence of *ortho*-borylation in phthalimide and naphthalimide, due to the inability of their carbonyls to adopt the required conformation for such non-covalent contacts with the ligand (Figures S20–S22).

Calculations also predicted that borylation of toluene would occur at the *meta* position, with both ligands **L2** and **L9** (Figure S18). The absence of the benzamide group destabilizes the *ortho* borylation TS with **L9** by ca. 5 kcal mol^{-1}. These predictions are in consonance with the experimental observations (Table S4), and further demonstrate the crucial role of outer-sphere interactions in both reactivity and *ortho*-regioselectivity. Loss of regioselectivity was also predicted and experimentally verified for the borylation of benzonitrile, whose cyano group cannot engage in the non-covalent interactions described for the benzamide group (Figures S19, S27 and S28).

Besides these unusual substrate-bipyridine interactions, calculations revealed an intriguing trend: in all cases entropy opposes and sometimes even supersedes enthalpy as the regioselectivity determining factor. Hence, relative activation enthalpies ($\Delta\Delta H^{\ddagger}$) always favor the *ortho* pathways, while the *meta* orientation is driven by entropy ($-T\Delta\Delta S^{\ddagger}$) (Figure S23).

Conclusion

In summary, we have discovered that the introduction of CF_3 groups at position 5 of bipyridine ligands (Ligand **L9**), triggers a complete change in regioselectivity in the iridium-catalyzed borylations of benzamides, from *meta/para* to *ortho*. Importantly, the presence of the amide directing group is critical to observe reactivity, which provides exquisite selectivity in polysubstituted and heteroaromatic substrates. This represents a substantial advantage with respect to other methods based on different ligand types.

Experimental data together with DFT calculations on the CF_3 and non-CF_3 containing ligands support a canonical Ir^{III}/Ir^{V} mechanism with a rate-determining C–H activation. Calculations suggest that the regioselectivity of the reactions stems from a subtle interplay of enthalpic and entropic contributions. While the *ortho* orientation tends to be penalized by steric and entropic factors, with 5-CF_3 substituted ligand **L9**, a significant enthalpic stabilization arises from unusual non-covalent interactions between the substrate's benzamide group and the polarized ring(s) of the bipyridine. This type of dispersion, non-covalent interactions

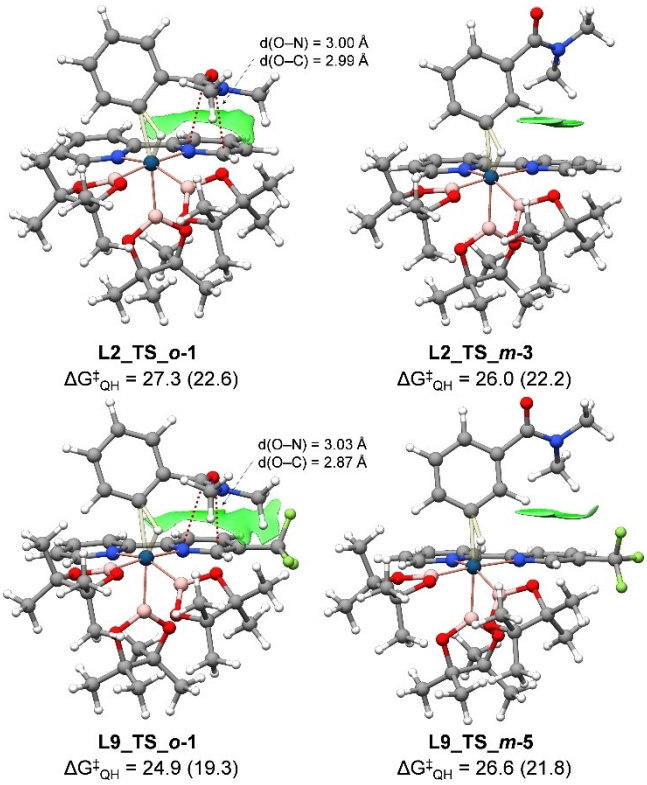

Figure 5. Substrate-ligand non-covalent interactions (NCI) occurring in low energy outer-sphere transition states (TS) calculated for the oxidative addition step between *N,N*-dimethylbenzamide (**1a**) and Ir^{III}(ligand)$(Bpin)_3$ (ligand = **L2** and **L9**; ***o*** = *ortho*, ***m*** = *meta*). Activation free energies ($\Delta G^{\ddagger}_{QH}$) calculated with SMD_{THF} and IEF-PCM_{THF} (in parentheses) and M06/6-311G(2d,p) + SDD(Ir)//M06/6-31G(d) + LANL2DZ(Ir) are given in kcal mol^{-1}. Metal-ligand and breaking/forming C–H, Ir–C and Ir–H bonds are represented as pale red and yellow lines, respectively. Contacts between the substrate carbonyl O and bipyridine N and C atoms are represented as red dashed lines. Note the larger extension of non-covalent interactions[24] in the *ortho* transition states, especially with ligand **L9**.

has rarely been invoked and should be taken into account in the future for other types of chemical reactions.

Acknowledgements

This research was funded by AEI (Spain) through projects PID2019-106184GB-I00 (to J.L.M.), PID2021-125946OB-I00 and RTI2018-099592-B-C22 (to G.J.O) and Severo Ochoa Excellence Accreditations (CEX2021-001136-S and SEV-2016-0644 to CIC bioGUNE). D.M. thanks MECD for a FPU fellowship (FPU18/04495) and Fulbright España for a US-Spain Fulbright grant. C.V. and F.P. thank MINECO for Juan de la Cierva Formación (FJCI-2017-33168) and Incorporación (IJC2020-045506-I) funding. We also want to thank Xunta de Galicia (2015-CP082, ED431C-2021/25 and Centro Singular de Investigación de Galicia accreditation 2019-2022, ED431G 2019/03) and ERDF. The Orfeo-Cinqa network is also acknowledged. The authors thank Dr. M. Marcos and Dr. N. Atanes from CACTI (Universidade de Vigo) for their excellent technical assistance and essential contributions to the kinetic studies and the characterization of products.

Conflict of Interest

The authors declare no conflict of interest.

Data Availability Statement

The data that support the findings of this study are available in the Supporting Information of this article.

Keywords: Bipyridine Ligands · Borylation · C–H Activation · Iridium · Non-Covalent Interactions

[1] a) T. Gensch, M. N. Hopkinson, F. Glorius, J. Wencel-Delord, *Chem. Soc. Rev.* **2016**, *45*, 2900–2936; b) M. Gulías, J. L. Mascareñas, *Angew. Chem. Int. Ed.* **2016**, *55*, 11000–11019; *Angew. Chem.* **2016**, *128*, 11164–11184; c) R. H. Crabtree, A. Lei, *Chem. Rev.* **2017**, *117*, 8481–8482; d) D. F. Fernández, J. L. Mascareñas, F López, *Chem. Soc. Rev.* **2020**, *49*, 7378–7405; e) N. Y. S. Lam, K. Wu, J. Q. Yu, *Angew. Chem. Int. Ed.* **2021**, *60*, 15767–15790; *Angew. Chem.* **2021**, *133*, 15901–15924; f) U. Dutta, S. Maiti, T. Bhattacharya, D. Maiti, *Science* **2021**, *372*, 6543; g) T. Dalton, T. Faber, F. Glorius, *ACS Cent. Sci.* **2021**, *7*, 245–261; h) E. Fernández, *Topics in Organometallic Chemistry*, Springer, Cham, **2021**, ISBN 978-3-030-69083-0.

[2] a) Z. Chen, B. Wang, J. Zhang, W. Yu, Z. Liu, Y. Zhang, *Org. Chem. Front.* **2015**, *2*, 1107–1295; b) C. Sambiagio, D. Schönbauer, R. Blieck, T. Dao-Huy, G. Pototschnig, P. Schaaf, T. Wiesinger, M. F. Zia, J. Wencel-Delord, T. Besset, B. U. W. Maes, M. Schnürch, *Chem. Soc. Rev.* **2018**, *47*, 6603–6743; c) L. Ping, D. S. Chung, J. Bouffard, S. Lee, *Chem. Soc. Rev.* **2017**, *46*, 4299–4328.

[3] a) G. Meng, N. Y. S. Lam, E. L. Lucas, T. G. Saint-Denis, P. Verma, N. Chekshin, J. Q. Yu, *J. Am. Chem. Soc.* **2020**, *142*, 10571–10591; b) V. K. Tiwari, M. Kapur, *Org. Biomol. Chem.* **2019**, *17*, 1007–1026.

[4] a) "Boronic Acids: Preparation and Applications": D. G. Hall, *Organic Synthesis and Medicine*, Wiley-VCH, Weinheim, **2005**; b) S. Namirembe, J. P. Morken, *Chem. Soc. Rev.* **2019**, *48*, 3464–3474; c) S. Darses, J. P. Genet, *Chem. Rev.* **2008**, *108*, 288–325; d) D. Leonori, V. K. Aggarwal, *Acc. Chem. Res.* **2014**, *47*, 3174–3183; e) E. C. Neeve, S. J. Geier, I. A. I. Mkhalid, S. A. Westcott, T. B. Marder, *Chem. Rev.* **2016**, *116*, 9091–9161; f) R. Bisht, C. Haldar, M. M. M. Hassan, M. E. Hoque, J. Chaturvedi, B. Chattopadhyay, *Chem. Soc. Rev.* **2022**, *51*, 5042–5100; g) C. Haldar, M. E. Hoque, J. Chaturvedi, M. M. M. Hassan, B. Chattopadhyay, *Chem. Commun.* **2021**, *57*, 13059–13074.

[5] a) S. A. Iqbal, J. Pahl, M. J. Ingleson, *Chem. Soc. Rev.* **2020**, *49*, 4564–4591; b) Y. Kuroda, Y. Nakao, *Chem. Lett.* **2019**, *48*, 1092–1100; c) Y. Li, X. Wu, *Angew. Chem. Int. Ed.* **2020**, *59*, 1770–1774; *Angew. Chem.* **2020**, *132*, 1786–1790; d) P. Nguyen, H. P. Blom, S. A. Westcott, N. J. Taylor, T. B. Marder, *J. Am. Chem. Soc.* **1993**, *115*, 9329–9330.

[6] a) T. M. Boller, J. M. Murphy, M. Hapke, T. Ishiyama, N. Miyaura, J. F. Hartwig, *J. Am. Chem. Soc.* **2005**, *127*, 14263–14278; b) H. Tamura, H. Yamazaki, H. Sato, S. Sakaki, *J. Am. Chem. Soc.* **2003**, *125*, 16114–16126.

[7] a) J. F. Hartwig, *Chem. Soc. Rev.* **2011**, *40*, 1992–2002; b) J. F. Hartwig, *Acc. Chem. Res.* **2012**, *45*, 864–873; c) L. Xu, G. Wang, S. Zhang, H. Wang, L. Wang, L. Liu, J. Jiao, P. Li, *Tetrahedron* **2017**, *73*, 7123–7157; d) J. S. Wright, P. J. H. Scott, P. G. Steel, *Angew. Chem. Int. Ed.* **2021**, *60*, 2796–2821; *Angew. Chem.* **2021**, *133*, 2830–2856; e) G. R. Genov, J. L. Douthwaite, S. K. Lahdenperä, D. C. Gibson, R. J. Phipps, *Science* **2020**, *367*, 1246–1251; f) M. T. Mihai, B. D. Williams, R. J. Phipps, *J. Am. Chem. Soc.* **2019**, *141*, 15477–15482.

[8] a) S. Kawamorita, H. Ohmiya, K. Hara, A. Fukuoka, M. Sawamura, *J. Am. Chem. Soc.* **2009**, *131*, 5058–5059; b) T. Ishiyama, H. Isou, T. Kikuchi, N. Miyaura, *Chem. Commun.* **2010**, *46*, 159–161; c) F. Xu, O. M. Duke, D. Rojas, H. M. Eichelberger, R. S. Kim, T. B. Clark, D. A. Watson, *J. Am. Chem. Soc.* **2020**, *142*, 11988–11992.

[9] a) A. J. Roering, L. V. A. Hale, P. A. Squier, M. A. Ringgold, E. R. Wiederspan, T. B. Clark, *Org. Lett.* **2012**, *14*, 3558–3561; b) A. Ros, R. Fernandez, J. M. Lassaletta, *Chem. Soc. Rev.* **2014**, *43*, 3229–3243; c) A. Ros, B. Estepa, R. López-Rodríguez, E. Alvarez, R. Fernández, J. M. Lassaletta, *Angew. Chem. Int. Ed.* **2011**, *50*, 11724–11728; *Angew. Chem.* **2011**, *123*, 11928–11932; d) R. Bisht, B. Chattopadhyay, *J. Am. Chem. Soc.* **2016**, *138*, 84–87.

[10] J. Jover, F. Maseras, *Organometallics* **2016**, *35*, 3221–3226.

[11] a) B. Ghaffari, S. M. Preshlock, D. L. Plattner, R. J. Staples, P. E. Maligres, S. W. Krska, R. E. Maleczka, M. R. Smith, *J. Am. Chem. Soc.* **2014**, *136*, 14345–14348; b) G. Wang, L. Liu, H. Wang, Y. S. Ding, J. Zhou, S. Mao, P. Li, *J. Am. Chem. Soc.* **2017**, *139*, 91–94; c) M. E. Hoque, M. M. M. Hassan, B. Chattopadhyay, *J. Am. Chem. Soc.* **2021**, *143*, 5022–5037; d) M. M. Mahamudul Hassan, B. Mondal, S. Singh, C. Haldar, J. Chaturvedi, R. Bisht, R. B. Sunoj, B. Chattopadhyay, *J. Org. Chem.* **2022**, *87*, 4360.

[12] a) C. Haldar, M. E. Hoque, R. Bisht, R. Chattopadhyay, *Tetrahedron Lett.* **2018**, *59*, 1269–1277; b) Y. Kuninobu, T. Torigoe, *Org. Biomol. Chem.* **2020**, *18*, 4126–4134; c) K. M. Engle, T.-S. Mei, M. Wasa, J. Q. Yu, *Acc. Chem. Res.* **2012**, *45*, 788–802; d) A. Unnikrishnan, R. B. Sunoj, *Chem. Sci.* **2019**, *10*, 3826–3835; e) H. J. Davis, R. J. Phipps, *Chem. Sci.* **2017**, *8*, 864–877; f) A. Fernández-Figueiras, M. A. Ravutsov, S. P. Simeonov, *ACS Omega* **2022**, *7*, 6439–6448.

[13] a) P. C. Roosen, V. A. Kallepalli, B. Chattopadhyay, D. A. Singleton, R. E. Maleczka, Jr., M. R. Smith III, *J. Am. Chem. Soc.* **2012**, *134*, 11350–11353; b) R. B. Smith, R. Bisht, C. Haldar, G. Pandey, J. E. Dannatt, B. Ghaffari, R. E. Maleczka, Jr., B. Chattopadhyay, *ACS Catal.* **2018**, *8*, 6216–6223.

[14] B. Chattopadhyay, J. E. Dannatt, I. L. Andujar-De Sanctis, K. A. Gore, R. E. Maleczka, D. A. Singleton, M. R. Smith, *J. Am. Chem. Soc.* **2017**, *139*, 7864–7871.

[15] a) H. L. Li, Y. Kuninobu, M. Kanai, *Angew. Chem. Int. Ed.* **2017**, *56*, 1495–1499; *Angew. Chem.* **2017**, *129*, 1517–1521; b) H.-L. Li, M. Kanai, Y. Kuninobu, *Org. Lett.* **2017**, *19*, 5944–5947.

[16] Q. Zheng, C. F. Liu, J. Chen, G. W. Rao, *Adv. Synth. Catal.* **2020**, *362*, 1406–1446.

[17] S. Bai, C. Bheeter, J. Reek, *Angew. Chem. Int. Ed.* **2019**, *58*, 13039–13043; *Angew. Chem.* **2019**, *131*, 13173–13177.

[18] a) A. Collado, M. A. Esteruelas, F. López, J. L. Mascareñas, E. Onate, B. Trillo, *Organometallics* **2010**, *29*, 4966–4974; b) D. Fernández, M. Gulías, J. L. Mascareñas, F. López, *Angew. Chem. Int. Ed.* **2017**, *56*, 9541–9545; *Angew. Chem.* **2017**, *129*, 9669–9673.

[19] a) Y. Kuninobu, H. Ida, M. Nishi, M. Kanai, *Nat. Chem.* **2015**, *7*, 712–717; b) R. Bisht, M. E. Hoque, B. Chattopadhyay, *Angew. Chem. Int. Ed.* **2018**, *57*, 15762–15766; *Angew. Chem.* **2018**, *130*, 15988–15992.

[20] A. G. Green, P. Liu, C. A. Merlic, K. N. Houk, *J. Am. Chem. Soc.* **2014**, *136*, 4575–4583.

[21] R. Pepin, C. Schmitz, G.-B. Lacroix, P. Dellis, C. Veyrat, U.S. Patent US5342835A, August 30, **1994**.

[22] S. Kozuch, S. Shaik, *Acc. Chem. Res.* **2011**, *44*, 101–110.

[23] "Natural Bond Orbital Methods": F. Weinhold in *Encyclopedia of Computational Chemistry, Vol. 3* (Ed.: P. v. R. Schleyer), Wiley, New York, **1998**, pp. 1792–1811.

[24] E. R. Johnson, S. Keinan, P. Mori-Sanchez, J. Contreras-Garcia, A. J. Cohen, W. Yang, *J. Am. Chem. Soc.* **2010**, *132*, 6498–6506.

[25] Deposition Numbers 2095587 (for **2a**), 2095584 (for **2ao**), and 2095495 (for **2ap**) contains the supplementary crystallographic data for this paper. These data are provided free of charge by the joint Cambridge Crystallographic Data Centre and Fachinformationszentrum Karlsruhe Access Structures service.

Manuscript received: October 4, 2022
Accepted manuscript online: January 5, 2023
Version of record online: January 24, 2023